RESEARCH PAPER

PCCP
www.rsc.org/pccp

The influence of a sugar-phosphate backbone on the cisplatin-bridged BpB′ models of DNA purine bases. Quantum chemical calculations of Pt(II) bonding characteristics

Michal Zeizinger,[a] Jaroslav V. Burda*[a] and Jerzy Leszczynski[b]

[a] *Department of Chemical Physics and Optics, Faculty of Mathematics and Physics, Charles University, Ke Karlovu 3, 121 16 Prague 2, Czech Republic*
[b] *Department of Chemistry, Jackson State University, 1325 J.R. Lynch Street, Jackson, Mississippi 39217-0510, USA*

Received 5th January 2004, Accepted 10th March 2004
First published as an Advance Article on the web 29th April 2004

The optimised structures of *cis*-$[Pt(NH_3)_2$-1,2-d{BpB′}$]^{2+}$ (B and B′ are guanine and adenine bases in all four combinations) were determined at the B3LYP/6-31G(d) level of calculations. The optimised parameters of the $[Pt(NH_3)_2$-{GpG}$]^{2+}$ complex are in very good agreement with the experimental data. The RMS of the predicted molecular parameters from the crystal structure is approximately 1.0 Å, even less than the difference between several experimental structures which are available in the NDB database. For the obtained reference geometries, an estimation of the bond dissociation energies (BDE), stabilisation energies ΔE^{stab}, and ΔE^{stex} together with the natural bond orbital population analysis (NBO) and MO analyses were performed using the MP2/6-31+G(d) method. The Pt–N7 bond is always stronger in the case of 3′-end base than for the 5′-end one. The highest abundance of a Pt-adduct to GpG, known from experiment, was confirmed by the predicted highest stabilisation of this complex. Also experimentally revealed, 20% of Pt{ApG} bridges simultaneously with practically no occurrence of Pt{ApA}, and this is in qualitative correspondence with the computed stabilisation. The explanation of the negligible occurrence of Pt{GpA} could originate in the kinetic and/or sterical conditions in the DNA chain since the monofunctional platinated complex contains exclusively guanine. Then if adenine is present above guanine (at the 5′-end), the N7 position of adenine is in close proximity of the second leaving group of cisplatin which increases the probability for the formation of Pt-{ApG}.

Introduction

Since Rosenberg *et al.*'s[1] discovery of the anticancer activity of cisplatin many platinum compounds involving both Pt(II) and Pt(IV) were explored. As a consequence cisplatin analogues of the second and third generations were found to be more active or less toxic for the human body. Carboplatin is one of the most often used drugs.[2] However, cisplatin serves still as a "benchmark" for the estimation of their activity. Also, the final adduct of cisplatin, carboplatin and some other platinum drugs includes the same *cis*-$[Pt(NH_3)_2$-1,2-d{GpG}$]^{2+}$ fragment or its derivatives. The molecular structure of this complex was solved for the first time by the Dickerson group with a resolution of 2.6 Å.[3] A similar structure, which contains the cisplatin G–Pt–G bridge,[4] was described with the same resolution. The distortion of DNA under the influence of cisplatin was revealed by Lilley.[5] In addition, the structure of the interstrand cisplatin bridge was published.[6] Recently also the oxaliplatin 1,2-d(GpG) intrastrand cross-link in a DNA oligomer was found.[7] Some other platinum complexes were crystallized and described.[8,9] The Lippard group was able to prepare and solve the crystal structure of a DNA oligomer with cisplatin and HMG-protein.[10,11]

Six-coordinate platinum(IV) complexes were also extensively explored.[12–16] These complexes are relatively stable and can be passed through the digestive tract. After absorption in the bloodstream, they are metabolised and form four-coordinate Pt(II) cisplatin analogues.[17] A summary of the current state in the treatment of platinum drugs can be found in the studies of Wong and Giandomenico[18] and Reedijk.[19] In another work, Reedijk demonstrates the competition between S-donor ligands and DNA.[20] The interstrand cross-linked binding of DNA bases with platinum was studied in detail by Brabec *et al.*[21] The quarternary platinum complexes in solution were studied by Sigel and Lippert.[22] The reaction rates for the hydration of cis/tranplatin were also explored.[23,24] Several conformers of the cisplatin adduct to GpG with different phosphodiester backbones were examined by the Marzilli group,[25] where an impressive combination of NMR (^{1}H and ^{31}P), CD spectroscopy, and MM and MD calculations was presented.

A comparison of platinum–guanine complexes with other selected metal–guanine cations was also published.[26] Interestingly, other groups explore the anticancer activity of some other transition metals.[27–31]

As to theoretical calculations, individual conformers of cis/transDDP were investigated by Pavankumar *et al.*[32] The DFT method was used in a study by Wysokinski and Michalska[33] for a comparison of the structure and vibration spectra of cisplatin and carboplatin. Mispairs in DNA caused by different stabilisations of rare tautomers after platination on the N4 site of cytosine were explored by Šponer *et al.*[34] and the N7 site of guanine and adenine in the works.[35,36] The transition states for chloride ligand replacement by water and guanine were studied by Chval and Šip.[37] The complex of cisplatin with 1,2-d(GpG) bases was examined by Carloni *et al.*[38] where also some hydration aspects of cisplatin were treated using Car–Parrinello MD simulations. The influence of N7 platination on the strength of the N9-C1′ glycosyl bond of purine bases was also revealed in this study.[39] DFT techniques with the VTZP basis set were used recently by Deubel[40] to compare affinities of cisplatin to S-sites and N-sites of amino acids and DNA bases. His results are in very good accord with our previous calculations on the

DOI: 10.1039/b317052g

thermodynamics of platinum complex hydration.[41–43] Cundari *et al.*[44] developed new force field parameters for platinum which enable the usage of classical molecular simulation of extended DNA models.

As mentioned above, despite the differences in leaving substituents which vary among some of the drugs based on cisplatin analogues, there are common features related to their products when diammine-Pt(II) binds to DNA chains. Here the most common product is the Pt-bridged complex with two guanines, cis[Pt(NH_3)$_2$-1,2-d(GpG)]$^{2+}$. Some other intrastrand coordinations occur less frequently, namely with the 1,2-d(ApG) and 1,3-d(GpXpG) bases sequences. However, the coordination to 1,2-d(ApA) or 1,2-d(GpA) were observed only very rarely. Recently we performed a study of untethered purine bases where some geometry discrepancy was noticed in the *cis*-[Pt(NH_3)$_2$ (N7,N7′-diguanine)]$^{2+}$ fragment due to a missing phosphate backbone. The present study reveals that these discrepancies are not important when the binding energy is considered. Moreover, this extended model has basic importance for establishing the proper reference geometry as is demonstrated by comparison of the obtained results with crystal structures.

Computational details

Optimisation of square-planar complexes of *cis*-[Pt(NH_3)$_2$-1,2-d(BpB′)]$^{2+}$ were performed using the hybrid Becke3LYP functional[45] with the 6-31G(d) basis set. B and B′ represent all possible combinations of adenine and guanine bases. Stuttgart energy-averaged relativistic pseudopotentials were used to describe the Pt[46] and P[47] atoms. The Pt valence basis set was extended with a set of diffuse functions $\alpha_s = 0.0075$, $\alpha_p = 0.013$, $\alpha_d = 0.025$ and with optimised polarisation functions $\alpha_f = 0.98$.[41]

Because of a possible comparison with previous calculations, the sugar-phosphate moiety had to be kept neutral. Therefore, the charge on the phosphate group was compensated by an additional proton. Other possibilities were also considered, namely neutralisation by a Na^+ cation. The optimisation of the considered systems with the cation led, however, to very soft potential energy surfaces which made the calculations even more computationally demanding. For this reason a much more localized O–H interaction was finally preferred. The same "neutralisation procedure" was also applied in some other papers where the phosphate moiety was treated (*e.g.*, refs. 48 and 49) All of the complexes were considered as 2+ charged species in the singlet electronic ground state.

Analogous with our previous work,[50] single-point calculations utilizing the 2nd order perturbation theory (MP2) were performed on the final optimised structures. Complex stabilisation energies and bond dissociation energies for individual ligands were computed at the MP2(frozen core)/6-31G(d) level with the inclusion of basis set superposition error (BSSE) by the Boys–Bernardi counterpoise method.[51]

The stabilisation energy is defined as

$$\Delta E^{\mathrm{stab}} = -\left[E^{\mathrm{complex}} - \sum_i E^i(\mathrm{BSSE})\right] \qquad (1)$$

where E^i(BSSE) labels individual parts of the complex. Ghost functions are located on the remaining atoms outside the given part of the complex. There were two different energy analyses performed on the final complexes: (a) global analysis which treats the whole complexes as they were optimised and (b) kernel analysis which deals with structures of reduced complexes where the sugar-phosphate moiety was omitted and where the N9 sites were anchored by hydrogens. Their bond lengths and angles were taken from our previous work.[50] The kernel analysis was treated within basis sets extended by diffuse functions (6-31+G(d)). This results in a better description of the bonding relation in the vicinity of the Pt atom. Also, a comparison with optimised *cis*-[Pt(NH_3)$_2$BB′]$^{2+}$ complexes (where purine bases were untethered by a sugar-phosphate backbone) from the previous study would be possible. In the kernel analysis, complexes were treated as five-part species: the Pt^{2+} cation and four ligands. The modified stabilisation energies E^{stex} which exclude the sterical repulsion of the ligands were evaluated. Here, instead of a sum of total energies of individual ligand, the energy of complex-optimised structure without the central Pt atom is used:

$$\Delta E^{\mathrm{stex}} = -(E^{\mathrm{complex}} - E^{\mathrm{L_1,\ldots,L_4}}(\mathrm{BSSE}) - E^{\mathrm{Pt}}(\mathrm{BSSE})] \qquad (2)$$

A similar formula to eqn. (1) was utilized for the bond dissociation energy (BDE) of the ligands where the energies of both parts (ligand and the rest of complex) were also BSSE-corrected. It is expected that errors of energy determination should remain under 5 kcal mol^{-1} with such a treatment.

In the global analyses, the complexes are consider as four-part species since both Pt–N7 bonds have to be split off simultaneously. Therefore only ΔE^{stex} and the energy of complex cleavage into two parts (both bases with a sugar-phosphate and Pt(NH_3)$_2^{2+}$) were evaluated. In the same way, the simultaneous cleavage of both unlinked bases was done on the smaller (kernel) part of the complexes so that the influence of the sugar-phosphate moiety could be elucidated.

The structures of DNA sequences with a Pt adduct were found in the NDB database (http://ndbserver.rutgers.edu/NDB). In refs. 4 and 9, intrastrand Pt bridges in DNA purine bases (GpG) were solved and published. A comparison of the corresponding structures was performed by XTALVIEW program (http://www.sdsc.edu/CCMS/Packages/XTALVIEW), and individual RMS's are discussed in the section with geometry parameters.

All calculations were performed with the quantum chemical program package Gaussian 98.[52]

Results and discussion

The optimisation procedure started from the known geometry of the crystal structure of the intrastrand [Pt(NH_3)$_2$-1,2-d(GpG)]$^{2+}$ complex.[4] This structure has sugar puckering on both ends in the 3-endo modes, and both Pt–N7 bonds exhibit pronounced deviation from the guanine planes (153 and 143 deg) which causes only minor deviation from unperturbed parallel guanine planes. Also the platinum ligands remain in planar arrangement which is contrary to another (newer) crystal structure[10] where pyramidal distortion is visible. In the optimised structures of Pt{GpG} and Pt{ApA}, sugar puckering preserves the 3-endo mode on the 3′-end but reveals a symmetrical twist $C_{2'}$-exo-$C_{3'}$-endo on the 5′-end. Mixed Pt{GpA} and Pt{ApG} complexes also posses the 3-endo mode on 3′-end but an unsymmetrical $^3T_2$ twist (with minor $C_{2'}$-exo) pucker on the 5′-end.[53] All final structures are displayed in Fig. 1. When a comparison between the original Takahara and optimised Pt{GpG} structure was performed, RMS values of 0.994 and 0.976 were obtained. A slightly worse result was obtained for Ohndorf's structure (RMS = 1.116). On the other hand, mutual comparison between both experimental structures leads to RMS = 1.157 and 1.173 which gives justification for the plausibility of our structures. All four structures exhibit a similar H-bonding pattern (with three H-bonds): two of them involve the sugar 5-hydroxy group at the 5′-end, P–O...H–O(5′) and O(5′)...H–C(8) (for atom numbering see Scheme 1). The third H-bond connects the electronegative X6-atom of the base at the 3′-end and the proximate ammine ligand. The values of the H-bond lengths are collected in Table 1. In the Pt{ApA} complex an additional H-bond from the other ammine-ligand to O(5′) occurs. The other complexes

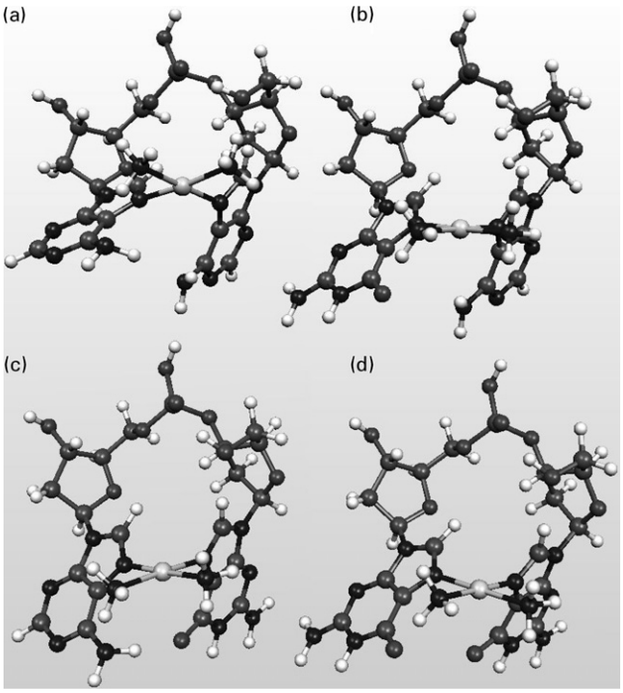

Fig. 1 Optimised geometries of all four Pt{BpB′} complexes. (a) Pt{ApA}, (b) Pt{ApG}, (c) Pt{GpA}, and (d) Pt{GpG}.

have these ammine ligands substantially further from the sugar moiety. In the case of the Pt{GpA} complex, interbase O6...H(N6) H-bonding can be seen. This type of H-bond was observed already in PtAG complexes with untethered DNA bases.[50] However, it was slightly shorter (about 0.08 Å) because of better relaxation of the bases. Remaining interbase H-bonds were broken during the optimisation process.

Another general geometrical feature revealed in this study concerns the deviation the of Pt–N_7 bond out of the base plane. Usually Pt–N_7 bonds are located nearly in the base plane at the 3′-end side. On the opposite 5′-end, the most remarkable deviation is noticeable in the Pt{ApA} complex, approximately 20 degrees (*cf.* last part of Table 1).

As to bond distances in the vicinity of the Pt atom, coordination of Pt-ammine is shorter in the cis position to 3′-end since this ligand is involved in H-bonding to the base. In this way, some nitrogens in ammonium have slightly larger electron density available for Pt-donation. An additional interbase

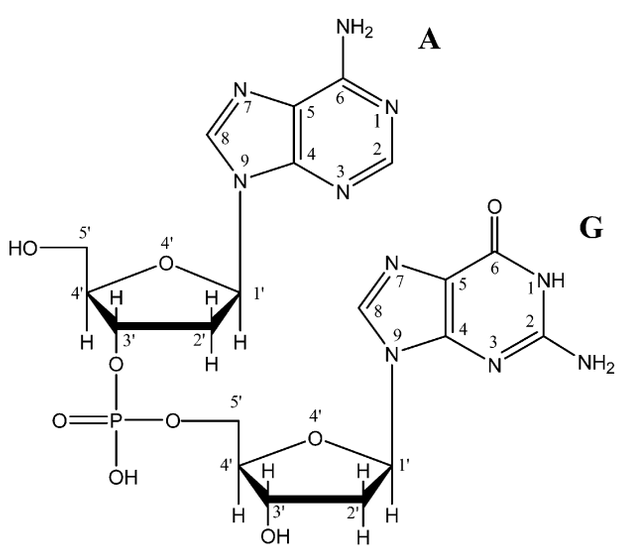

Scheme 1 Atom numbering in ApG fragment.

Table 1 Selected geometry parameters of *cis*-[$Pt(NH_3)_2$-1,2-d(BpB)]$^{2+}$ complexes optimised at B3LYP/6-31G(d) (bond lengths in Å and angles in °)

	GpG	ApG	GpA	ApA
Pt-bonds				
Pt–N7(5′)	2.038	2.036	2.026	2.057
Pt–N7(3′)	2.049	2.050	2.042	2.042
Pt–N(5′a)	2.088	2.090	2.092	2.097
Pt–N(3′a)	2.081	2.087	2.094	2.093
H-bonds				
H(a1)···O6	1.763	1.810	2.081	2.039
H(O5′)···O(P)	1.894	1.874	1.878	1.820
H(C8)···O5′	2.034	2.014	2.009	1.967
H(N6)···O6		3.174	2.095	3.515
H(a2)···O5′				2.216
Torsions				
N9-C8-N7-Pt (5′)	175.0	170.0	169.7	158.0
N9-C8-N7-Pt (3′)	169.0	173.0	178.0	174.4

H-bond (from the same N6 site of adenine) weakens the ammine-adenine H-bond resulting in comparable Pt–N(ammine) distances in the Pt{GpA} complex. The Pt–N7 distances are systematically shorter at 5′-end which also partially weakens the ammine ligand in the *cis*-3′-end position due to trans-effect. The Pt–N7 distances for the 3′-end bases exhibit remarkable length conservation. The longer Pt–N7(5′) bond in the Pt{ApA} complex is probably a result of the greater deviation of the Pt–N7 bond from the base-plane which partially aggravates the donor-acceptor bonding relations (for details see Table 1 and Fig. 1). It is interesting to compare Pt{GpG} with the optimised PtGG complex where the symmetrical geometry results from the missing backbone. Despite the unlinked bases, the larger Pt–N7 distance was obtained there (about 0.03Å for the 5′-end and 0.02Å for the 3′-end). The reason can be seen in the higher mutual repulsion of both bases in symmetrical arrangement (*cf.* discussion below and Table 2). For other PtBB′ complexes, the differences of the Pt–N distances remain under 0.01 Å.

Comparing the geometrical changes in DNA bases, one concludes that practically all of the distances were unchanged (within 0.005 Å). The larger values of the C8-H bonds (by about 0.01 Å) reflect H-bonding to the sugar O5′. According

Table 2 Kernel analysis - MP2/6-31+G(d) stabilisation energies ΔE^{stab} and ΔE^{stex}, BDE of Pt-ligand, deformation energies ΔE(def) and comparison with optimised PtBB systems and global analysis – ΔE^{stex} and BDE at MP2/6-31G(d) level (in kcal mol^{-1})

Kernel analysis	GG	AG	GA	AA
ΔE^{stex}	−549.5	−527.3	−529.4	−502.2
ΔE^{stab}	−524.1	−508.2	−513.3	−482.8
BDE(5′B)	−98.9	−83.4	−111.7	−82.6
BDE(3′B)	−108.7	−117.7	−95.7	−96.4
BDE(5′a)	−67.1	−69.2	−68.5	−67.2
BDE(3′a)	−73.8	−74.2	−73.1	−74.9
ΔE(def)	7.2	6.3	8.6	7.1
ΔE(def,5′B)	3.0	2.1	3.6	2.7
ΔE(def,3′B)	3.7	3.7	4.7	4.0
Pt{BpB} *vs.* Pt{BB}				
ΔBDE(5′B)	−4.3	−11.6	−0.8	−7.2
ΔBDE(3′B)	5.4	5.3	0.7	−1.0
ΔBDE(5′a)	−5.8	1.0	0.3	−2.1
ΔBDE(3′a)	1.0	1.2	0.2	0.7
Global analysis				
ΔE^{stex}	−589.2	−568.7	−568.1	−552.0
ΔE(BpB-Pt(NH_3)$_2$)	−276.0	−257.8	−259.2	−244.8
ΔE(BB-Pt(NH_3)$_2$)	−251.0	−229.7	−233.4	−205.8

to these prolongations, it can be guessed that these bonds are relatively strong despite a "C–H" H-bond character. The other (more pronounced) changes concern C6-X6 (X=O, N) bonds of the 5′-end base. They are shortened (by about 0.02 Å) in comparison with complexes without a sugar-phosphate moiety. This clearly points to missing interbase H-bonds in ApA and ApG complexes and the ammine$\cdots O_6$ bond in GpG complex in the 5′-end bases. Thus, no electron density of the X6 atom is transferred out of the C6-X6 bond. From this point nothing was changed in the Pt{GpA} complex where the interbase H-bond remains. Thus, no change can be noticed comparing the untethered and linked complexes.

Energy analyses of the kernel parts are summarized in the first part of Table 2. As could be expected, the largest stabilisation energy is predicted for the Pt{GpG} complex. Surprisingly, the Pt{ApG} conformer is less stable than its Pt{GpA} analogue. This can be regarded as a consequence of the relatively strong Pt–N7 bond of the 5′-end guanine which is stronger by more than 10 kcal mol^{-1} than the same dative bond in the Pt{GpG} complex. Also, when sterical repulsion is neglected, the Pt atom is more firmly coordinated to the {GpA} structure (where this repulsion is the smallest). From Table 2, it can be seen that the 3′-end bases are coordinated to the metal cation more strongly than the 5′-end bases. The higher strength is partially supported by the H-bonds between ammine-ligand and the X6 position of the base. It can be seen that these Pt–N7 bonding energies do not correlate with the corresponding bond lengths which are longer for the 3′-end bases in all guanine-containing complexes (*cf.* the above discussion). Indirect confirmation of the larger BDE of the 3′-end bases is also noticeable from the deformation energies. Larger deformation reflects stronger interaction. Interestingly, the strongest Pt-guanine coordination occurs in the Pt{ApG} complex where all of the BDE's reach their maximal values. The BDE energies of ammine ligands are practically independent of the base (approximately 68 kcal mol^{-1} for the ligand in the cis position to the 3′-end and up to 74 kcal mol^{-1} for the 5′-end ligand). This is also in good accord with the conclusion concerning the stronger 3′-end base coordination to Pt which influences the corresponding ammine ligand through the trans-effect.

In the middle section of Table 2, a comparison with the previous model is made. Clearly, the energy differences are not large. The BDE of the Pt-guanine bonds in Pt{GpG} points to the disproportion of the "averaged" Pt–N_7 coordination energy of the symmetrical $[Pt(NH_3)_2(N_7\text{-guanine})_2]^{2+}$ complex. The decreased BDE of NH_3(*cis* to 5′-end) is connected with the vanishing of the corresponding H-bond interaction. The relatively large difference for the Pt{ApG} complex reflects the larger geometry reorientation since the PtGA complex was used for comparison. Thus, an increase of BDE for Pt-guanine at the 3′-end in the Pt{ApG} complex occurs simultaneously with the decrease for the 5′-end adenine. The good results for the Pt{GpA} complex justify the much simpler model used previously. In the Pt{ApA} complex, the BDE for the geometry with linked bases does not have the same strength of BDE for isolated AA bases, and this fact is a result of a geometry relaxation which is worse for adenine bases under sugar-phosphate linkage mainly at the 5′-end.

From the global energy analyses of the whole complexes, the influence of a sugar-phosphate backbone can be elucidated. Here only the stabilisation energy without sterical repulsion ΔE^{stex} and the energy of simultaneous splitting of both Pt–N_7 bonds were estimated. In the bottom part of Table 2, a comparison of BDE(Pt{BpB}) and BDE(PtBB) at MP2/6-31G(d) is presented. The higher stabilisation, in the case of nucleotides, can be explained by the additional electrostatic interaction of the negatively charged phosphate group and metal cation. This term represents about 25 kcal mol^{-1} in all guanine-containing complexes. Surprisingly, the substantially large influence of the backbone is remarkable in the case of diadenine, about 40 kcal mol^{-1}. The same conclusion follows from a comparison of the ΔE^{stex} energies despite the slightly different basis sets used.

We are aware of the fact that treatment of the $Pt(NH_3)_2^{2+}$ species in the frame of BDE calculations is not completely justified since the electron configurations differ in four-ligated and two-ligated complexes, and this also affects the electronic energies. Nevertheless, from previous calculations, it can be seen that the same trends follow from the reaction energies where the regular purely four-ligated square-planar Pt(II) complexes are treated with the BDE calculations according to the formula above. One aspect of the calculations of the Pt{ApG} and Pt{GpA} complexes deals with the order of stability of both systems. While the Pt{ApG} complex is presented exclusively in the experimental data, our calculations reveal Pt{GpA} as being the more stable complex. Only at the DFT level optimisation, the total energy of the Pt{ApG} system is negligibly higher (approximately 0.5 kcal mol^{-1}). Nevertheless, this value is within the range of computational error. At all single-point MP2 calculations performed using the obtained reference geometries, all types of energy comparisons (total energies, stabilisation ΔE^{stab} or ΔE^{stex} energies) slightly prefer the Pt{GpA} complex.

Estimation of stacking interaction is not performed in this study since the geometries of the DNA bases were changed only marginally in comparison with the previous model without the sugar-phosphate backbone; the same energies for this interaction can be expected.[50,54] Moreover, it is clear that the role of H-bonding will be overestimated in a gas phase environment and with stacking interaction suppressed.[55,56]

NBO population analyses were performed for Pt complexes with both untethered bases and with bases connected by a sugar-phosphate backbone. Table 3 provides a comparison of the electron densities at different levels of calculation: MP2 and B3LYP, with and without a sugar-phosphate connection. The stability of NBO analysis is demonstrated in this example. All five central atoms exhibit the same trend when involved in various combinations of the DNA bases. Also, only marginal influence of the sugar-phosphate on the electron distribution in the vicinity of the Pt atom is noticeable.

From MO analyses, basically all conclusions found in a previous work were reproduced here. However, an interesting feature concerns the fact that HOMO is always π orbital-localized on the 5′-end base (the 168th MO for the Pt{GpG} complex, in Fig. 2d) leaving the corresponding 3′-end-base π orbital slightly

Table 3 NBO population analyses of Pt and the closest N atoms (in *e*)

	GpG	ApG	GpA	ApA
NBO at MP2/6-31G(d)				
Pt	0.675	0.655	0.666	0.657
5G-N7	−0.494	−0.517	−0.490	−0.520
3G-N7	−0.481	−0.488	−0.502	−0.504
5NH3	−1.036	−1.038	−1.039	−1.046
3NH3	−1.048	−1.048	−1.051	−1.045
NBO at B3LYP/6-31G(d)				
Pt	0.705	0.686	0.696	0.684
5G-N7	−0.519	−0.543	−0.517	−0.546
3G-N7	−0.507	−0.516	−0.527	−0.534
5NH3	−1.039	−1.042	−1.043	−1.054
3NH3	−1.054	−1.055	−1.057	−1.050
NBO at B3LYP/6-31G(d) untethered BB				
Pt	0.708	0.688	0.699	0.688
5G-N7	−0.515	−0.538	−0.512	−0.541
3G-N7	−0.504	−0.513	−0.524	−0.529
5NH3	−1.041	−1.043	−1.044	−1.051
3NH3	−1.052	−1.053	−1.054	−1.049

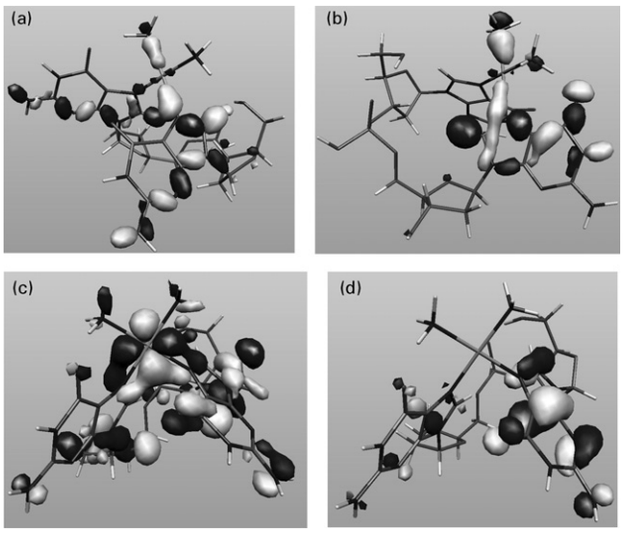

Fig. 2 Important MO of the Pt{GpG} complex. (a) 114th donation from 5′-end guanine, (b) 116th donation from 3′-end guanine, (c) 139th back donation from d_{xy} AO to p AOs on the N7 of both guanines, and (d) 168th HOMO localized on 5′ end guanine.

lower in energy (0.2–0.5 eV). Thus, it is in accord with the larger BDE of Pt–N7 for the 3′-end base. This fact also points to the larger reactivity of the 5′-end base. Another confirmation for a stronger Pt–N7 of the 3′-end base can be seen in the larger donation from the base σ orbital to the virtual $d_{x^2-y^2}$ AO of Pt. This σ-donation is asymmetric, more pronounced in the case of the 3′-end base. The 114th MO represents a smaller donation from N7 of the 5′-end to Pt (smaller expansion coefficients on the N7 and Pt atoms) than in the case of the 116th MO (*cf.* the 114th and 116th MOs, in Fig. 2a and b). Back-donation is realized by only one MO d_{xy} (139th MO, in Fig. 2c) and is substantially more symmetrical.

The HOMO/LUMO gap was found to be approximately 4.5 eV (slightly smaller in the case of adenine) at the B3LYP level. These values substantially differ from the analogous data of a recent study of similar complexes.[38]

Conclusions

Different Pt-bridged models with tethered DNA purine bases were investigated in this study. For the calculations, only HH (head-to-head) orientation of the bases was chosen. It was found that the optimised geometry (at the B3LYP/6-31G(d) computational level) of Pt{GpG} is in very good correspondence to the experiments. It does not deviate substantially from the known crystal parameters. The deviations remain within a range of error in which various experimental structures differ.

Pt bonding is more pronounced to the 3′-ended base than to 5′-ended base. This is confirmed by the values of the BDE energies, lower partial charges on the N7 site (better donation), and direct donation from MO analysis.

Calculated preferences for GpG over ApG, GpA, and ApA are in qualitative agreement with the literature[57] (about 65% abundance of G–Pt–G bridges). According to the experimental data, one should expect that 20% of Pt{ApG} bridges simultaneously with practically no occurrence of Pt{GpA}. This finding is not in agreement with the calculated results, but an explanation of this fact is found in the kinetic and/or sterical conditions in the DNA chain. The first interaction, which creates the monofunctional platinated complex, leads predominately to a Pt-adduct with guanine. Then if adenine is present above guanine (at the 5′-end), the N7 position of adenine is in close proximity of the second leaving group (H_2O or Cl) of cisplatin which increases the probability for the formation of Pt-{ApG}.[58]

Using the Boltzmann distribution law, the relative occurrence of individual complexes in a DNA environment should be confirmed. However, differences of several orders might be received based on the stabilisation energies. It can be expected that the consideration of a correct environment will cause a large screening not considered in "*in vacuo*" calculations which means that the energy differences for the Pt–N7 bond between guanine and adenine (mainly based on the Coulomb interaction) will be decreased as mentioned in our previous works where a series of calculations with different total charges of the complexes were performed.[35,36] It was demonstrated that passing from 2+ charged to neutral complexes, the energies of the Pt–N7 bonds for guanine and adenine are decreased to a very similar limit (about 50 kcal mol^{-1}). Thus, according to the experimentally known distribution, the screening factors (or "external" total charge) which would reproduce the corresponding differences in stabilisation energies for the considered environment can be estimated. The influence of a sugar-phosphate chain onto Pt-bridged complexes can be seen in the higher stability of the examined complexes or in comparison of the ΔE(BpB–Pt$(NH_3)_2$) and ΔE(BB-Pt$(NH_3)_2$) rows in Table 2. This fact can be explained mainly by the relatively large coulomb interaction between the positively charged Pt atom and the negative phosphate group. Despite the increased interactions, the basic trends remain unchanged. The most pronounced effect is visible in the diadenine complex where the sugar-phosphate backbone exhibits the largest influence due to larger polarisability as was already mentioned several times in other studies where the trans-effect of guanine and adenine was explored.

The conclusions of our previous results on the interaction with untethered DNA bases remain practically unchanged from an energetical point of view. Even the relatively large sterical repulsion in the diguanine complexes, which was discussed as an artefact of the model used, was changed only partially (by 3 kcal mol^{-1}). Moreover, the repulsion of the diadenine complex increased by about 4 kcal mol^{-1} due to the geometrical restrictions of the sugar-phosphate backbone.

We believe that the present study highlights the details of the interactions between Pt complexes and DNA bases, reveals the particulars of geometrical arrangement, and undoubtedly confirms previously found trends.

Acknowledgements

This study was supported by Charles University grants GAUK 259/2002/B_CH/MFF (MZ) and 181/2002/B_CH/MFF (JVB), and NSF MŠMT ČR ME-517 grant (JVB). Partial support was also obtained by NSF grant OSR-94527857 and by the Office of Naval Research, grant No. N00014-95-1-0049. Special thanks is given to the computational resources from Meta-Centres in Prague, Brno, and Pilsen for excellent access to their supercomputer facilities and their kind understanding. We would also like to acknowledge the Mississippi Supercomputing Research Center which supported many of the calculations.

References

1 B. Rosenberg, L. Van Camp, J. L. Trosko and V. H. Mansour, *Nature*, 1969, **222**, 385.
2 W. Kaim, B. Schwederski, *Bioinorganic Chemistry: Inorganic Elements in the Chemistry of Life*, John Wiley & Sons Ltd, Chichester, England, 1994.
3 R. M. Wing, P. Pjura, H. R. Drew and R. E. Dickerson, *EMBO J.*, 1984, **3**, 1201.
4 P. M. Takahara, A. C. Rosenzweig, C. A. Frederick and S. J. Lippard, *Nature*, 1995, **377**, 649.

5 D. M. J. Lilley, *J. Biol. Inorg. Chem.*, 1996, **1**, 189.
6 F. Coste, J. M. Malinge, L. Serre, W. Shepard, M. Roth, M. Leng and C. Zelwer, *Nucleic Acids Res.*, 1999, **27**, 1837.
7 B. Spingler, D. A. Whittington and S. J. Lippard, *Inorg. Chem.*, 2001, **40**, 5596.
8 A. P. Silverman, W. Bu, S. M. Cohen and S. J. Lippard, *J. Biol. Chem.*, 2002, **277**, 49 743.
9 G. N. Parkinson, G. M. Arvantis, L. Lessinger, S. L. Ginell, R. Jones, B. Gaffney and H. M. Berman, *Biochemistry*, 1995, **34**, 15 487.
10 U.-M. Ohndorf, M. A. Rould, Q. He, C. O. Pabo and S. J. Lippard, *Nature*, 1999, **399**, 708.
11 E. R. Jamieson and S. J. Lippard, *Chem. Rev.*, 1999, **99**, 2467.
12 J. Kašparková, F. S. Mackay, V. Brabec and P. J. Sadler, *J. Biol. Inorg. Chem.*, 2003, **8**, 741.
13 S. Choi, S. Delaney, L. Orbai, E. J. Padgett and A. S. Hakemian, *Inorg. Chem.*, 2001, **40**, 5481.
14 H. Junicke, C. Bruhn, R. Kluge, A. S. Serianni and D. Steinborn, *J. Am. Chem. Soc.*, 1999, **121**, 6232.
15 R. Song, K. M. Kim, S. S. Lee and Y. S. Sohn, *Inorg. Chem.*, 2000, **39**, 3567.
16 M. Watanabe, M. Kai, S. Asanuma, M. Yoshikane, A. Horiuchi, A. Ogasawara, T. Watanabe, T. Mikami and T. Matsumoto, *Inorg. Chem.*, 2001, **40**, 1496.
17 L. R. Kelland, B. A. Murrer, G. Abel, C. M. Giandomenico, P. Mistry and K. R. Harrap, *Cancer Res.*, 1992, **52**, 822.
18 E. Wong and C. M. Giandomenico, *Chem. Rev.*, 1999, **99**, 2451.
19 J. Reedijk, *Chem. Commun.*, 1996, **7**, 801.
20 J. Reedijk, *Chem. Rev.*, 1999, **99**, 2499.
21 V. Brabec, K. Neplechova, J. Kasparkova and N. Farell, *J. Biol. Inorg. Chem.*, 2000, **5**, 364.
22 H. Sigel, B. Song, G. Oswald and B. Lippert, *Chem. Eur. J.*, 1998, **4**, 1053.
23 J.-L. Jestin, B. Lambert and J.-C. Chottard, *J. Biol. Inorg. Chem.*, 1998, **3**, 515.
24 J. Arpalahti, in *Metal Ions in Biological Systems*, ed. A. Sigel and H. Sigel, Marcel Dekker, Inc., New York, Basel, Hong Kong, 1996, vol. 32, pp. 380.
25 K. M. Williams, T. Scarcia, G. Natile and L. G. Marzilli, *Inorg. Chem.*, 2001, **40**, 445.
26 B. Song, J. Zhao, R. Griesser, C. Meiser, H. Sigel and B. Lippert, *Chem. – Eur. J.*, 1999, **5**, 2374.
27 H. Chen, J. A. Parkinson, S. Parsons, R. A. Coxal, R. O. Gould and P. Sadler, *J. Am. Chem. Soc.*, 2002, **124**, 3064.
28 J. Malina, O. Novakova, B. K. Keppler, E. Alessio and V. Brabec, *J. Biol. Inorg. Chem.*, 2001, **6**, 435.
29 H. T. Chifotides, K. M. Koshlap, L. M. Perez and K. R. Dunbar, *J. Am. Chem. Soc.*, 2003, **125**, 10 703.
30 H. T. Chifotides, K. M. Koshlap, L. M. Perez and K. R. Dunbar, *J. Am. Chem. Soc.*, 2003, **125**, 10 714.
31 O. Nováková, H. Chen, O. Vrána, A. Rodger, P. J. Sadler and V. Brabec, *Biochemistry*, 2003, **42**, 11 544.
32 P. N. Pavankumar, P. Seetharamulu, S. Yao, J. D. Saxe, D. G. Reddy and F. H. Hausheer, *J. Comput. Chem.*, 1999, **20**, 365.
33 R. Wysokinski and D. Michalska, *J. Comp. Chem.*, 2001, **22**, 901.
34 J. Šponer, J. E. Šponer, L. Gorb, J. Leszczynski and B. Lippert, *J. Phys. Chem. A*, 1999, **103**, 11 406.
35 J. V. Burda, J. Šponer and J. Leszczynski, *J. Biol. Inorg. Chem.*, 2000, **5**, 178.
36 J. V. Burda, J. Šponer and J. Leszczynski, *Phys. Chem. Chem. Phys.*, 2001, **3**, 4404.
37 Z. Chval and M. Šíp, *J. Mol. Struct. (THEOCHEM)*, 2000, **532**, 59.
38 P. Carloni, M. Sprik and W. Andreoni, *J. Phys. Chem. B*, 2000, **104**, 823.
39 M.-H. Baik, R. A. Friesner and S. J. Lippard, *J. Am. Chem. Soc.*, 2002, **124**, 4495.
40 D. V. Deubel, *J. Am. Chem. Soc.*, 2002, **124**, 5834.
41 J. V. Burda, M. Zeizinger, J. Sponer and J. Leszczynski, *J. Chem. Phys.*, 2000, **113**, 2224.
42 M. Zeizinger, J. V. Burda, J. Šponer, V. Kapsa and J. Leszczynski, *J. Phys. Chem. A*, 2001, **105**, 8086.
43 J. V. Burda, M. Zeizinger and J. Leszczynski, *J. Chem. Phys.*, 2004, **120**, 1253.
44 T. R. Cundari, W. Fu, E. W. Moody, L. L. Slavin, L. A. Snyder, S. O. Sommerer and T. R. Klinckman, *J. Phys. Chem.*, 1996, **100**, 18 057.
45 A. D. Becke, in *Modern Electronic Structure Theory*, ed. D. Yarkony, World Scientific, Singapore, 1995.
46 D. Andrae, U. Haussermann, M. Dolg, H. Stoll and H. Preuss, *Theor. Chim. Acta*, 1990, **77**, 123.
47 M. Dolg, U. Wedig, H. Stoll and H. Preuss, *J. Chem. Phys.*, 1987, **86**, 866.
48 O. V. Shishkin, L. Gorb, O. A. Zhikol and J. Leszczynski, *J. Biomol. Struct. Dynam.*, 2004, **21**, 537.
49 J. Šponer, M. Sabat, L. Gorb, J. Leszczynski, B. Lippert and P. Hobza, *J. Phys. Chem. B*, 2000, **104**, 7535.
50 J. V. Burda and J. Leszczynski, *Inorg. Chem.*, 2003, **42**, 7162.
51 S. F. Boys and F. Bernardi, *Mol. Phys.*, 1970, **19**, 553.
52 M. J. Frisch, G. W. T., H. B. Schlegel, G. E. Scuseria, M., A. Robb, J. R. C., V. G. Zakrzewski, J. A. Montgomery, Jr., R. E. Stratmann, J. C., S. D. Burant, J. M. Millam, A. D. Daniels, K. N. Kudin, M. C. Strain, O. Farkas, J., V. B. Tomasi, M. Cossi, R. Cammi, B. Mennucci, C. Pomelli, C. Adamo, S. Clifford, J., G. A. P. Ochterski, P. Y. Ayala, Q. Cui, K. Morokuma, P. Salvador, J. J. Dannenberg, D. K. Malick, A. D. R. K. Raghavachari, J. B. Foresman, J. Cioslowski, J. V. Ortiz, A., G. Baboul, B. B. S. G. Liu, A. Liashenko, P. Piskorz, I. Komaromi, R. L. R. Gomperts, D. J. F. Martin, T. Keith, M. A. Al-Laham, C. Y. Peng, A. Nanayakkara, M. Challacombe, P. M. W. Gill, B. J., W. Chen, M. W. Wong, J. L. Andres, C. Gonzalez, M. Head-Gordon and J. A. Pople, *Gaussian 98 (Revision A.1x)*, Gaussian, Inc., Pittsburgh, PA, 2001.
53 W. Saenger, *Principles of Nucleic Acid Structure*, Springer-Verlag, New York, 1983.
54 J. Šponer, I. Berger, N. Špaèková, J. Leszczynski and P. Hobza, *J. Biomol. Struct. Dynam.*, 2000, 383.
55 M. Rueda, S. G. Kalko, F. J. Luque and M. Orozco, *J. Am. Chem. Soc.*, 2003, **125**(125), 8007.
56 S. A. Trygubenko, T. V. Bogdan, M. Rueda, M. Orozco, F. J. Luque, J. Sponer, P. Slavicek and P. Hobza, *Phys. Chem. Chem. Phys.*, 2002, **4**, 4192.
57 A. Eastman and N. Schulte, *Biochemistry*, 1988, **27**, 311.
58 A. Eastman, *Biochemistry*, 1985, **24**, 5027.

